

Effect of back-interface recombination velocity on surface photovoltage for GaAs photocathodes

LIANG CHEN^{a, b*}, YUNSHENG QIAN^b, XINLONG CHEN^b, RUI YANG^b, SHUQIN ZHANG^a

^a*Institute of Optoelectronics Technology, China Jiliang University, 310018, Hangzhou, China*

^b*Institute of Electronic Engineering & Optoelectronics Technology, Nanjing University of Science and Technology, 210094, Nanjing, China*

Varied doping structures of GaAs photocathodes have been proved to enhance quantum efficiency than uniform doping structure. As the value of active electrons is not only in close connection with the electron diffusion length, active layer thickness but also in connection with the back-interface recombination velocity. In consider of the back-interface recombination velocity, we deduced the modified equations of surface photovoltage for exponential doping structure and uniform doping structure. Through emulations, the exponential doping structure can reduce the decreasing trend of surface photovoltage than uniform doping structure along the back-interface recombination velocity growing. Through experiments and analysis, the influences of internal electric field for two structures were well discussed. This investigation can help to well study the varied doping structures and optimize the structure designs for GaAs photocathodes in the future.

(Received November 2, 2011; accepted November 23, 2011)

Keywords: GaAs photocathode, Surface photovoltage, Back-interface recombination velocity, Varied doping

1. Introduction

Negative-electron-affinity (NEA) GaAs photocathodes have already been found widespread applications in night vision image intensifiers and are potential sources for the next-generation electron accelerators due to their high spin polarization, low energy spread, and good emittance. The quantum efficiency of NEA GaAs photocathodes mainly depends on the performance of the material and the technique of preparation. In recent years, the varied doping structures design for GaAs photocathodes material has been the research hotspot, which can form an internal electric field by the Fermi-level leveling effect of the varied doping concentration in active layer of photocathode material and drive more photoelectrons to surface barriers through not only diffusion but also electric field drift. Though many researches have been carried out on the varied doping structure design by the help of spectral response after Cs-O activations, but the effect of back-interface recombination velocity (BIRV) for the performance of material has not been deeply studied restricted by the spectral response after Cs-O activation which is influenced not only by the properties of body materials but also by the Cs-O activation technology and structure of surface barriers [1]. As the surface photovoltage before Cs-O activation is only in connection with the properties of body materials, thus the parameters of body materials such as electron diffusion length, BIRV and so on can be exactly measured without the influence of Cs-O activation technology and structure of surface barriers after activation. So by means of surface photovoltage, we can well study the influence of BIRV for GaAs photocathodes [2-3]. In this paper, the equations of surface photovoltage for exponential doping structure (EDS)

and uniform doping structure (UDS) were well deduced. Through emulations, the influences of BIRV for two structures were evidently fitted. In order to verify the emulating results, two materials of different structures were designed by our own. Through experiments and calculations for two materials, the differences of two materials on internal electric field were deeply discussed.

2. Principle on surface photovoltage

The EDS means that the p-type doping concentrations in the active layer of photocathode vary from body to surface according to the following equation of Eq.1 [4].

$$N(x) = N_0 \exp(-Ax) \quad (1)$$

Where x is the distance between a point in the active layer and the back interface, A is the exponential doping coefficient, N_0 is the initial doping concentration of the back interface, and $N(x)$ is the doping concentration at the distance of x .

As a result of EDS, a constant built-in electric field direction from back interface to surface is formed, which can be expressed as Eq.2 [5].

$$V(x) = \frac{k_0 T}{q} \ln \frac{N_0}{N(x)} = \frac{k_0 T}{q} \ln \frac{N_0}{N_0 \exp(-Ax)} = \frac{k_0 T A x}{q} \quad (2)$$

Where k_0 is the Boltzmann constant, T is the absolute temperature, and q is the electronic charge. Thus, the

relationship between x and $V(x)$ is shown as Fig. 1 and the directional built-in electric field can drive photo-excited electrons to surface by electric drift.

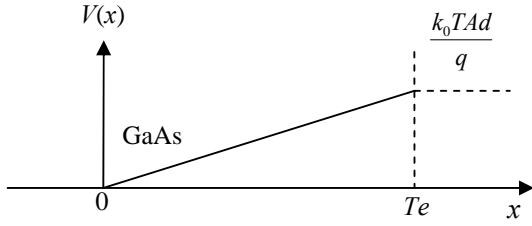


Fig. 1. Built-in electric voltage of exponential doping GaAs photocathodes.

As the electric field intensity is constant in doping active layer, a continuously downward band structure from the GaAs bulk to the surface is formed in the photocathodes as is shown in Fig. 2, where V_D and d_s are the energy value and depth for the surface band bending region, the \square and \parallel surface barriers are the results of Cs-O activation for GaAs photocathodes, E_C is the conduction band minimum, E_V is the valence band maximum, and E_F is the Fermi level.

$$D_n \frac{d^2 n(x)}{dx^2} - \mu |E| \frac{dn(x)}{dx} - \frac{n(x)}{\tau} + \alpha_{hv} I_0 (1-R) \exp[-\alpha_{hv}(T_e - x)] = 0 \quad (3)$$

So in consider of the internal electric field, the one-dimensional diffusion equation for the no equilibrium minority carriers of reflection-mode GaAs photocathodes is modified as Eq.3 [6], where D_n is the electron diffusion coefficient, τ is the electron lifetime, T_e is the active layer thickness, α_{hv} is absorption coefficient, S_V is the back-interface recombination velocity, μ is the electron mobility. Furthermore, the boundary conditions are given as Eq.4.

$$D_n \frac{dn(x)}{dx} - \mu |E| n(x) \Big|_{x=0} = S_V n(x) \Big|_{x=0}, n(T_e) = 0 \quad (4)$$

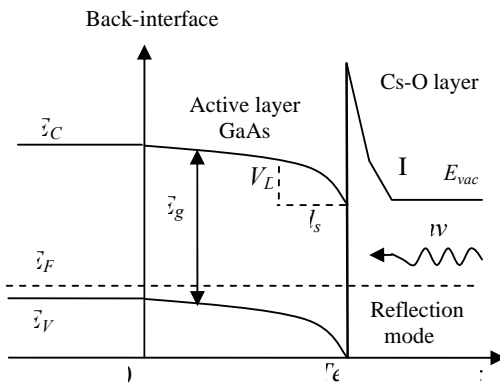


Fig. 2. Band structure for exponential doping GaAs photocathodes.

According to diode theory, the theory equations for surface photovoltage ΔV and photoelectron current at surface barriers J_w are shown as Eq.5 [7].

$$\Delta V = \frac{k_0 T}{q} \ln\left(1 + \frac{j_w}{c}\right), J_w = D_n \frac{dn(x)}{dx} \Big|_{x=T_e} \quad (5)$$

$$\Delta V = \frac{k_0 T I_0 (1-R) \alpha_{hv} L_D}{q c (\alpha_{hv}^2 L_D^2 - \alpha_{hv} L_E - 1)} \times \left\{ \frac{N(S - \alpha_{hv} D_n)}{M} \times \exp\left[\left(L_E / 2L_D^2 - \alpha_{hv}\right) T_e\right] - \frac{Q}{M} + \alpha_{hv} L_D + \alpha_{hv} L_D \right\} \quad (6)$$

Thus from Eq.3-5, the surface photovoltage equation for EDS can be deduced as the following equation Eq. 6 [8].

Where L_E is the electron drift length under electronic field and the coefficients in Eq.6 are shown as Eq. 7.

$$L_E = \mu |E| \tau = \frac{q |E|}{k_0 T} L_D^2, N = \sqrt{L_E^2 + 4L_D^2}, S = S_V + \mu |E|$$

$$M = \frac{ND_n}{L_D} \cosh\left(\frac{NT_e}{2L_D}\right) + \left(2SL_D - \frac{D_n L_E}{L_D}\right) \sinh\left(\frac{NT_e}{2L_D}\right) \quad (7)$$

$$Q = SN \cosh\left(\frac{NT_e}{2L_D}\right) + (S L_E + 2D_n) \sinh\left(\frac{NT_e}{2L_D}\right)$$

Thus the surface photovoltage equation of UDS can also be got from Eq.6 when the value of $E(x)$ is set to be zero as the following equation of Eq. 8.

$$\Delta V = \frac{k_0 T I_0 (1-R) \alpha_{hv} L_D}{q c (\alpha_{hv}^2 L_D^2 - 1)} \times \left\{ \frac{(S_V - \alpha_{hv} D_n) \exp(-\alpha_{hv} T_e)}{(D_n/L_D) \cosh(T_e/L_D) + S_V \sinh(T_e/L_D)} - \frac{S_V \cosh(T_e/L_D) + (D_n/L_D) \sinh(T_e/L_D)}{(D_n/L_D) \cosh(T_e/L_D) + S_V \sinh(T_e/L_D)} + \alpha_{hv} L_D \right\} \quad (8)$$

3. Experiments and analysis

Thus from above equations, we can draw the detailed emulations on the influence of BIRV for the surface photovoltage of GaAs photocathodes. For fitting the surface photovoltage curves for UDS, the coefficients in Eq.8 were set as $L_D=3 \mu\text{m}$, $D_n=120\text{cm}^2/\text{s}$, $T_e=3 \mu\text{m}$. Thus the finally emulating curves for UDS were got as Fig. 3, where the values of surface photovoltage were normalized [9].

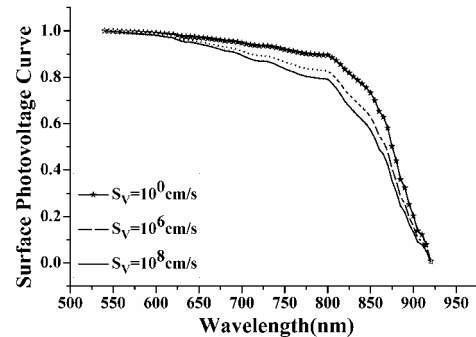


Fig. 3. Surface photovoltage curves for UDS.

For fitting the surface photovoltage curves for EDS, the coefficients in Eq. 7 were set as $A=1.5\mu\text{m}^{-1}$, $L_D=3\mu\text{m}$, $D_n=120\text{cm}^2/\text{s}$, $T_e=3\mu\text{m}$. Thus the final emulating waves for exponential doping photocathodes were got as Fig. 4, where the values of surface photovoltage were also normalized.

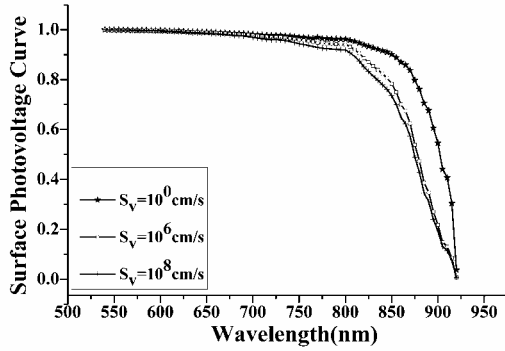


Fig. 4. Surface photovoltage curves for EDS.

For fitting the surface photovoltage curves for EDS, the coefficients in Eq. 7 were set as $A=1.5\mu\text{m}^{-1}$, $L_D=3\mu\text{m}$, $D_n=120\text{cm}^2/\text{s}$, $T_e=3\mu\text{m}$. Thus the final emulating waves for exponential doping photocathodes were got as Fig. 4, where the values of surface photovoltage were also normalized.

From above emulations, we can find that the surface photovoltage values decrease deeply along the BIRV rising for two doping structures. But the EDS can reduce the decreasing trend along the wavelength band than the UDS with the same value of BIRV. The reason is that the internal body electric field of EDS can drive more photoelectrons to surface barriers through diffusion and electric drift and reduce the influence of BIRV, while the internal electric field of UDS is almost zero by the result of same doping concentration in active layer [10].

0.35 μm , $1.0\times 10^{18}\text{cm}^{-3}$	1.60 μm , $1.0\times 10^{19}\text{cm}^{-3}$
0.30 μm , $1.7\times 10^{18}\text{cm}^{-3}$	
0.25 μm , $2.7\times 10^{18}\text{cm}^{-3}$	
0.20 μm , $4.0\times 10^{18}\text{cm}^{-3}$	
0.16 μm , $5.5\times 10^{18}\text{cm}^{-3}$	
0.13 μm , $7.0\times 10^{18}\text{cm}^{-3}$	
0.11 μm , $8.5\times 10^{18}\text{cm}^{-3}$	
0.10 μm , $1.0\times 10^{19}\text{cm}^{-3}$	
<i>p</i> -GaAs (100)	
<i>p</i> -GaAs (100)	

Fig. 5. Diagrams for photocathode materials of different doping structures.

In order to further verify the emulating results, we designed two different reflection-mode GaAs photocathode materials by molecular beam epitaxial (MBE) growth with *p*-type beryllium doping. The diagrams of detailed doping structures are shown in Fig. 5, where the doping concentration for the material of UDS is $1\times 10^{19}\text{cm}^{-3}$, the thickness of the epitaxial layer is 1.6 μm and the doping

concentrations for the material of EDS vary along the trend as is shown in Eq.1. Because the absolute exponential distribution is difficult to achieve by MBE technology, so the epitaxial layer for EDS was divided into eight sections separately along exponential doping distribution which satisfies $N_{\bar{0}}=1\times 10^{19}\text{cm}^{-3}$, $N(1.6)=1\times 10^{18}\text{cm}^{-3}$ and the doping coefficient $A \approx 1.44\mu\text{m}^{-1}$ [6]. Thus we can calculate the theoretical curves for two materials by the above deduced equations.

Before measuring the surface photovoltage curves, the GaAs photocathode materials were passed through acetone, hydrofluoric acid, absolute ethyl alcohol in turn for ultrasonic washing to above five minutes separately in order to wipe off the surface oxidation layers and impurities. When measuring process began, the samples were sandwiched between two indium-tin oxide (ITO) glass electrodes and putted into steel pool for shielding off sound, electromagnetism and other disturbing sources [10]. In order to avoid saturation phenomena, the irradiating light power on the sample was set at about 200 nW and the frequency of light chopper was set at 30 Hz which can ensure the surface photovoltage level to resume being same without light irradiating [11]. Through experiments, the surface photovoltage curves for two doping materials were well measured as are shown in Fig. 6. The fitting curves for two materials which were calculated along Eq.6 and Eq.8 are also shown in Fig. 7, where the values of surface photovoltage are normalized.

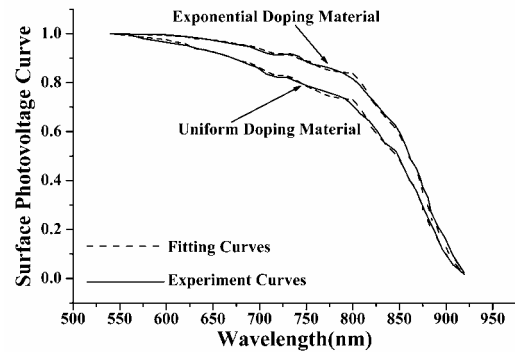


Fig. 6. Experimental and fitting curves for surface photovoltage.

The fitting parameters for two doping materials are shown in Table 1. We can find that though the doping thickness of two materials is the same value, the material of EDS can not only increase the electron diffusion length L_D but also reduce the back-interface recombination velocity S_v than the material of UDS [12].

Table 1. Fitting parameters for materials of EDS and UDS.

Material	$D_n(\mu\text{m}^2/\text{s})$	$T_e(\mu\text{m})$	$S_v(\mu\text{m}/\text{s})$	$L_D(\mu\text{m})$
EDS	1.2×10^{10}	1.6	1.2×10^{10}	2.1
UDS	1.0×10^{10}	1.6	1.0×10^{10}	1.3

As the main difference for two materials is the variation of doping concentration, the reason for the difference of parameters between two materials must mainly depend on the variation of internal electric field. Thus we should carry on a deep investigation on the internal band structure for two materials. Because the material of EDS is separated into eight sections with different doping concentration from high to low throughout the buck to surface, thus the different doping concentration can form band bending region at each different doping interface by the Fermi-level leveling effect [12]. The surface band bending energy V_D can be calculated by Eq. 9.

$$V_D \approx 2 \frac{k_0 T}{q} \ln \frac{N_d}{N_i} \quad (9)$$

Where k_0 is the Boltzmann's constant, T is the absolute temperature, q is the electronic charge, N_d is the surface-layer doping concentration, and N_i is the intrinsic carrier concentration. Because the surface-layer doping concentration of the material of EDS is $1 \times 10^{18} \text{cm}^{-3}$, which is less than that of UDS, so the surface band bending energy of exponential doping material is lower than that of the uniform doping material. Thus the reason for the surface photovoltage of exponential doping material being higher than that of uniform doping material is mainly determined by the internal band bending energy in active layers. Supposing that the actual carrier concentrations of the two adjacent sections are N_{A1} and N_{A2} respectively, where $N_{A1} > N_{A2}$, thus the band-bending energy qV_D due to the carrier concentration discrepancy is given as the following equation of Eq. 10 [13].

$$qV_D = E_{F2} - E_{F1} = (E_V + k_0 T \ln \frac{N_V}{N_{A2}}) - (E_V + k_0 T \ln \frac{N_V}{N_{A1}}) \quad (10)$$

Where E_{F1} is the Fermi level of high doping section, E_{F2} is the Fermi level of low doping section, k_0 is Boltzmann constant, T is absolute temperature, E_V is the valence band maximum, and N_V is the valence band density of states of GaAs. Thus we can get the final band-bending energy function as Eq. 11.

$$qV_D = k_0 T \ln \frac{N_{A1}}{N_{A2}} \quad (11)$$

Through calculations, the band-bending energy values between different doping layers in active layer for material of EDS were got as are shown in Tab.2, where section1 corresponds to the energy between the layers of doping concentration from $1.0 \times 10^{19} \text{cm}^{-3}$ to $8.5 \times 10^{18} \text{cm}^{-3}$. Section1 to section7 follows the sequence from the highest doping concentration to the lowest doping concentration [14].

Table 2. Band-bending energy between different doping layers of exponential doping material.

Unit (meV)						
Section	Section2	Section3	Section4	Section5	Section6	Section7
4.18	4.99	6.2	8.19	10.11	11.9	13.65

Because the uniform doping material has the same doping concentration in active layer, so it has no band bending energy caused by doping concentration. Because the band bending energy between different doping layers in EDS can drive more photo-excited electrons to the surface barriers through electric drift besides diffusion, thus the electron diffusion length and BIRV can be effectively increased which will finally improve the quantum efficiency for EDS than UDS.

4. Conclusion

In consider of the BIRV, we deduced the equations for surface photovoltage of EDS and UDS. Through emulations and experiments, we found that the material of EDS could well reduce the decreasing trend of surface photovoltage than that of UDS under the same BIRV. The reason is that the internal body electronic field of exponential doping material can not only increase the diffusion length, but also decrease the BIRV than uniform doping material. This research on the influence of BIRV for different doping structures can help to well study the internal body properties and optimize the varied doping structure designs for GaAs photocathodes in the future.

Acknowledgements

This work is supported by the National Natural Science Foundation of China under Grant No.60678043, 60871012.

References

- [1] I. Kudman, T. Seidel, J. Appl. Phys **33**, 771 (1962).
- [2] H. K. Pollehn, Adv. Electron. Electron Phys **64A**, 61 (1995).
- [3] L. I. Antonova, V. P. Denissov, Appl. Surf. Sci **111**, 237 (1997).
- [4] Z. Yang, B. K. Chang, J. J. Zou, J. J. Qiao, P. Gao, Y. P. Zeng, H. Li, Appl. Opti **46**, 7035 (2007).
- [5] J. Niu, Y. J. Zhang, B. K. Chang, Y. Zhi, Y. J. Xiong, Appl. Opti **48**, 5445 (2009).
- [6] J. Toušek, D. Kindl, J. Touškoá, S. Dolhov, J. Appl. Phys **89**, 460 (2001).
- [7] J. J. Zou, B. K. Chang, Y. Zhi, Y. Y. Zhang, J. L. Qiao, J. Appl. Phys **105**, 013714 (2009).
- [8] Y. Z. Liu, J. L. Moll, W. E. Spicer, Appl. Phys. Lett **17**, 60 (1970).
- [9] L. Chen, Y. S. Qian, B. K. Chang, Optoelectron. Adv. Mater. – Rapid Commun. **4**(12), 1967 (2010).
- [10] L. Chen, Y. S. Qian, Y. J. Zhang, B. K. Chang, Opt. Commun **284**, 4520 (2011).
- [11] J. J. Zou, B. K. Chang, Opt. Eng **45**, 054001 (2006).
- [12] F. Machuca, Z. Liu, J. R. Maldonado, S. T. Coyle, P. Pianetta, R. F. W. Pease, J. Vac. Sci. Technol. B **22**, 3565 (2004).
- [13] Y. J. Zhang, B. K. Chang, Z. Yang, J. Niu, Y. J. Xiong, F. Shi, H. Guo, Y. P. Zeng, Appl. Opti **48**, 1715 (2009).
- [14] Boreham. B. W, Newman. D. S. Höpel. D. S. Hora, J. Appl. Phys **78**, 5848 (1995).

*Corresponding author: sunembed@yahoo.com.cn